Materials Science Forum
ISSN: 1662-9752, Vol. 1185, pp 149-160
doi:10.4028/p-8jkHA8
© 2026 The Author(s). Published by Trans Tech Publications Ltd, Switzerland.
Submitted: 2026-01-19
Revised: 2026-02-11
Accepted: 2026-02-23
Online: 2026-04-15

Numerical Analysis of the Influence of a Movable Die on Joint Formation in Versatile Self-Piercing Riveting

Pia Katharina Kaimann[1,a*], Mathias Bobbert[1,b] and Gerson Meschut[1,c]

[1]Paderborn University, Pohlweg 47-49, 33098 Paderborn, Germany

[a]pia.kaimann@lwf.upb.de, [b]mathias.bobbert@lwf.upb.de, [c]gerson.meschut@lwf.upb.de
(*corresponding author)

Keywords: Self-piercing riveting, FEM, Versatility, Movable die.

Abstract. Self-piercing riveting (SPR) is a well-established joining technique in lightweight construction, as it enables the joining of different materials without requiring pre-drilling. However, the necessary adaptation of the rivet-die combination to the respective material and thickness combinations requires a large number of specific tool sets, which significantly limits the process's flexibility. To overcome these limitations, the versatile self-piercing riveting (V-SPR) was developed, which features enhanced punch actuation in combination with a multi-range-capable rivet [1]. In this context, the concept of a movable die was introduced, which enables an extended process window and adaptable joint formation. Kappe et al. presented initial studies demonstrating the potential of this approach [2]. However, a detailed numerical understanding of the underlying mechanisms remains lacking. This paper presents a numerical analysis of V-SPR with a movable die using a finite element (FE) model. The model includes deformable rivets, sheet metal materials and a kinematically controlled die with adjustable movement. A parameter study was conducted to analyse the influence of die movement on the material flow of the rivet and sheets, as well as joint formation. The simulations were validated using selected experimental data. The goal is to compare the joint geometries achieved with fixed and moving dies and expand the process windows of V-SPR. The results demonstrate that the movable-die concept significantly enhances the material flow of both the sheets and the rivet, resulting in a noticeably larger and more reliable interlock than what is achievable with V-SPR using a fixed die. The numerical analyses support the observations reported by Kappe et al. and extend them by providing a quantitative description of how die displacement influences the resulting interlock size. Moreover, the ability to precisely control the die movement makes it possible to join challenging sheet-metal combinations that are difficult to process with conventional setups, particularly in cases involving thicker sheet materials.

Introduction

Reducing CO_2 emissions has become a key objective in the automotive industry due to stricter environmental regulations and the EU's target of significantly cutting emissions by 2030 [3]. Alongside new drive concepts, lightweight construction remains one of the most effective strategies, as lowering vehicle mass directly reduces emissions [4]. Modern lightweight design increasingly relies on multi-material systems that combine materials with different properties to meet local load requirements. However, this material mix creates significant challenges for thermal joining methods, which often fail when joining dissimilar materials such as aluminium and high-strength steel due to metallurgical incompatibilities. For this reason, mechanical joining technologies, especially self-piercing riveting (SPR), have become essential, offering a reliable solution for joining diverse material combinations in automotive applications.

Self-piercing riveting (SPR) enables joining multiple layers, even of different materials, without pre-drilling, provided access is available from both sides. The process sequence is shown in Fig. 1. After positioning the components, the blank holder fixes the sheets. The rivet is then pressed into the die-side layer by the punch, cuts through it and takes up the punched-out remnant in the rivet shank. When the tool-side position is reached, the rivet is radially expanded and compressed by the die contour, creating a form-fitting and force-fitting closing head. After the return stroke of the punch

This article is an open access article under the terms and conditions of the Creative Commons Attribution (CC BY) license (https://creativecommons.org/licenses/by/4.0)

and blank holder, the connection remains fully formed. The process takes place in a single stroke, can be automated and is very reliable [5].

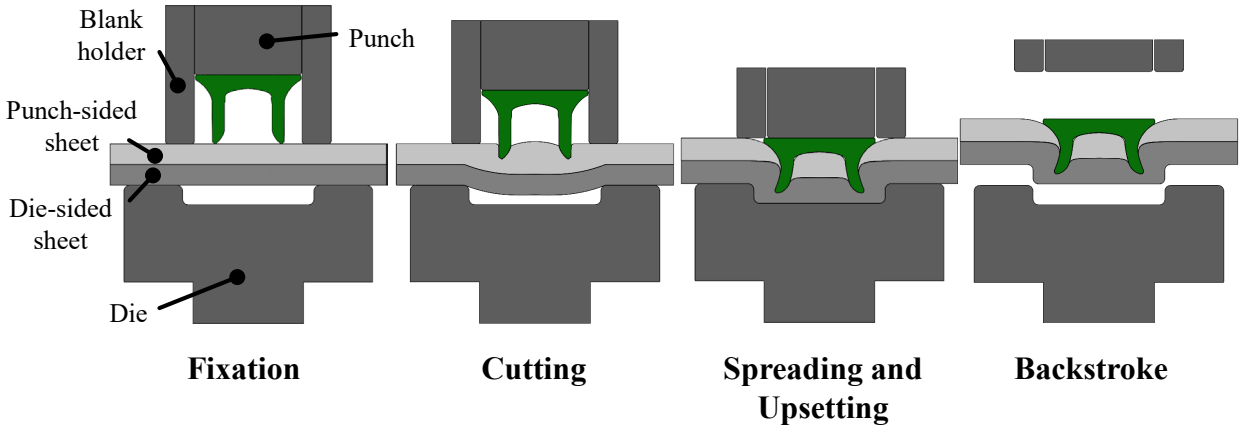

Fig. 1. Process sequence of the self-piercing riveting [5]

One restriction of SPR is the need to adapt the rivet–die combination to changing boundary conditions, such as variations in sheet thickness or material. This limitation has driven research toward more versatile and adaptable joining processes that enable broader applications. One such development is versatile self-pierce riveting (V-SPR), which combines extended tool kinematics with a multi-range capable rivet to join varying sheet thickness combinations without altering the rivet-die setup [1]. In contrast to conventional SPR, the punch-side tool is split into an inner and an outer punch. The process sequence is shown in Fig. 2. The inner punch first sets the rivet, after which the outer punch forms the rivet head to the respective sheet thickness, enabling robust joining even under fluctuating joining conditions.

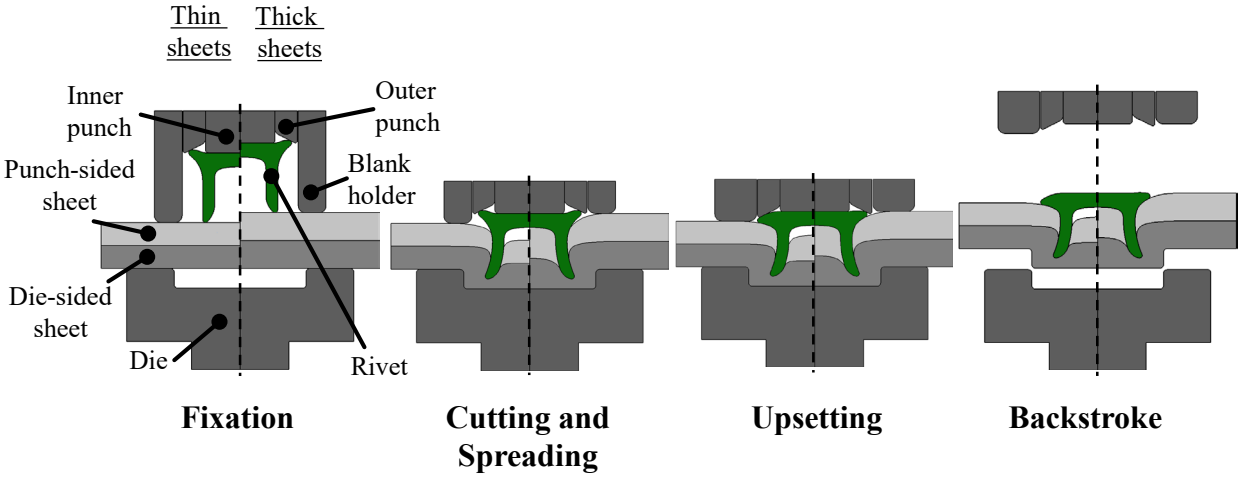

Fig. 2. Process sequence of the versatile self-piercing riveting [1]

Another approach to reducing rivet-die combinations is the use of a two-part die principle with a movable die element, as shown in [6]. Drossel and Jäckel (2014) were able to show that brittle aluminium material behaviour can be joined by movement in the bottom of the die [7]. Kappe et al. show that both a continuously lowering die bottom and subsequent embossing significantly increase the formation of the closing head. At the same time, material flow and stress states change, with a continuously lowering die bottom in particular generating increased compressive stresses in the slug and thus supporting rivet expansion. Subsequent stamping also improves the connection quality, but places a strain on the tools [2].

This study combines the V-SPR and the concept of a continuously descending die and numerically analyses the influence of different die movement sequences on joint formation, as shown in Fig. 3.

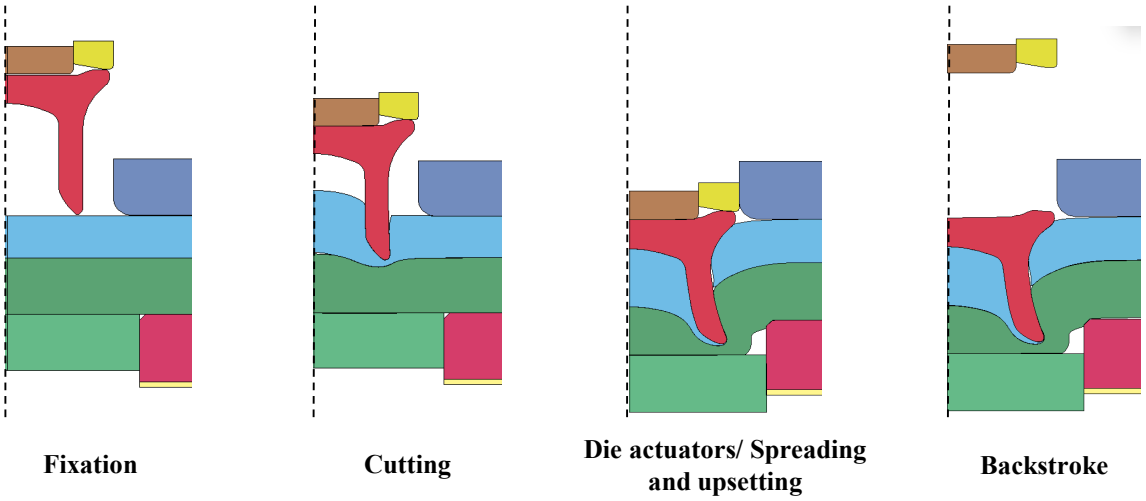

Fig. 3. Process sequence of the V-SPR with movable die

Experimental Procedure

The rivet, designed for use across multiple material ranges, is made from C35 B+Cr steel. The sheets are made of aluminium alloy EN AW 6014 in temper T4. The chemical compositions of both the rivet material and the EN AW 6014 alloy used in this study are listed in Table 1.

Table 1. Chemical composition properties of rivet material C35 B+Cr [8] and sheet materials EN AW-6014 temper T4 [9]

Chemical composition C35 B+Cr (weight %)									
Elements	Si	C	Cu	Mn	P	S	Cr	Mo	B
Min.		0.35		0.60					0.0008
Max.	0.3	0.40	0.25	0.90	0.025	0.025	0.3	-	0.005
Chemical composition EN AW-6014, T4 (weight %)									
Elements	Si	Fe	Cu	Mn	Mg	Cr	Zn	Ti	V
Min.	0.30			0.05	0.40				
Max.	0.60	0.35	0.25	0.20	0.80	0.20	0.10	0.10	0.10

For the joining operation, a setup is used that enables the inner and outer punches to move independently, as outlined earlier. As illustrated in Fig. 4, the upper tooling, consisting of both punch elements and the blank holder, and the lower tooling are mounted within a column-guided frame [10].

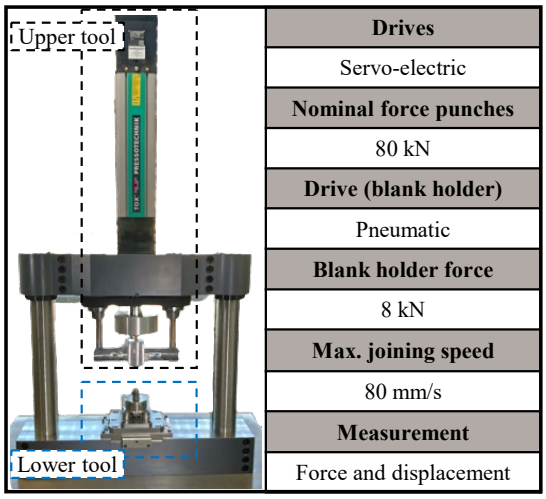

Drives
Servo-electric
Nominal force punches
80 kN
Drive (blank holder)
Pneumatic
Blank holder force
8 kN
Max. joining speed
80 mm/s
Measurement
Force and displacement

Fig. 4. Joining system with extended punch-sided tool actuator technology to process the multi-range capable self-piercing rivets [10]

Numerical simulation

To examine how a movable die affects joint formation in versatile self-piercing riveting, a two-dimensional axisymmetric simulation model was developed, as illustrated in Fig. 4. The approach builds on earlier work by KAPPE et al. [11]. The finite-element model was generated using the LS-Dyna simulation software and evaluated using an implicit solution strategy. The inner and outer punches were represented as elastic bodies to enable a detailed assessment of the forces generated during the operation. A displacement-controlled punch motion was imposed by constraining the corresponding nodes in the model. The inner punch moves at 9 mm/s. The movable die consists of a rigid die ring and a movable die base, both modelled as elastic parts, with their joining force measured in the lower area. The blank holder, implemented as a rigid body, applied a constant load throughout the entire procedure. Material behaviour was introduced using experimentally derived flow curves for the sheet and rivet material. Contact interactions between the rivet and sheets, as well as between the sheets themselves, were described using a static friction coefficient of 0.2 [12]. The punch-side sheet was cut according to a geometric criterion triggered by the prevailing process conditions.

FE-simulation – Relevant parameters	
Simulation software	LS-Dyna
Solver	smp_d_R910
Analysis	Implicit
Section	Shell
Element formulation	15 – Axissymmertric solid
Material seperation criterion	Geometrical
Process control	Displacement (Punches)
Punch feed direction	Y-Axis

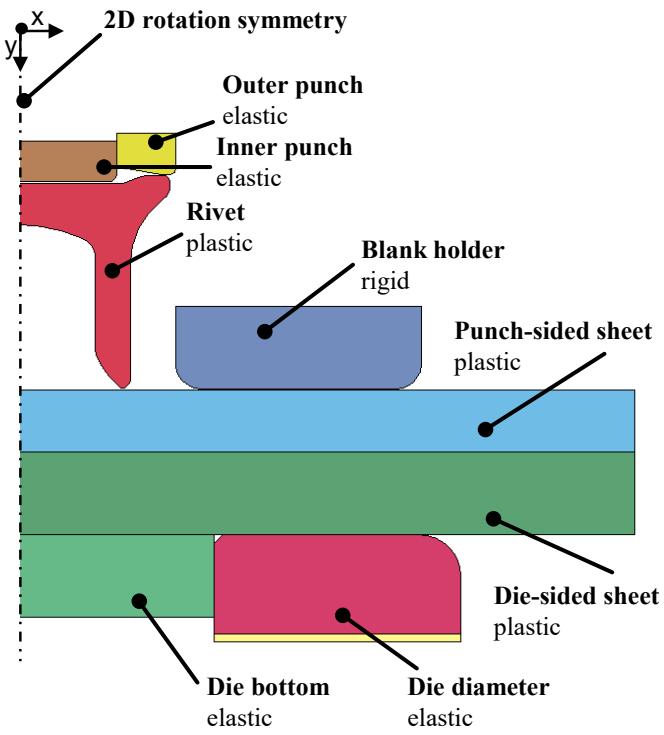

Fig. 5. Numerical setup of the V-SPR joining process

The numerical simulation was validated using the material thickness combination EN AW-6014 in 1.5 mm on the punch side and EN AW-6014 in 2.0 mm on the die side. Fig. 6 compares experimentally produced joints with corresponding simulation results, both in micrographs and in quality-relevant parameters such as interlock formation and the minimum die-sided material thickness. The visual comparison shows that the simulation captures the characteristic deformation behaviour of the sheets and the rivet, including the radial expansion of the rivet shank, the material flow into the interlock zone, and the thinning of the die-side sheet, with a high degree of fidelity. Likewise, the numerical predictions of the quality parameters closely align with the measured values, with only minor deviations. This agreement confirms that the model reliably represents the dominant physical mechanisms of the joining process and can therefore be used with confidence to analyse parameter influences and to explore process optimisation strategies.

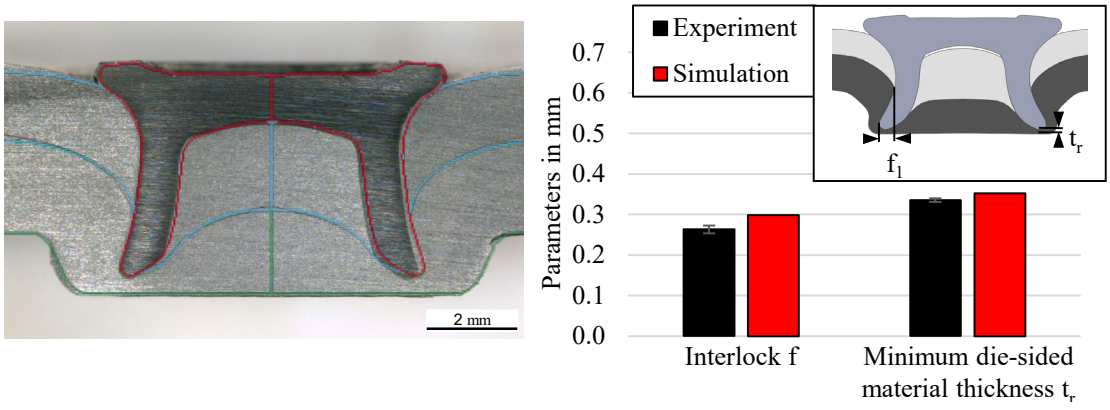

Fig. 6. Validation of material combination EN AW-6014 in 1.5mm in EN AW-6014 in 2.0 mm

Results and Discussion

To determine the influence of die movement on material flow and joint formation, a full factorial design of experiments (DoE) was set up (see Table 2). The following factors are varied: the thickness of the punch-side sheet metal, the thickness of the die-side sheet metal, the preset die depth at the

start time, the die velocity, and the start time of the die movement, depending on the total process duration. The quality-relevant parameters, interlock (f) and the minimal die-side material thickness (tr), were used as the response variables. The range of the start time of the die movement is based on the total time of the inner punch movement. The percentage increments are selected around the cutting process of the reference connections. The die velocity is set below the inner punch velocity so the die bottom can apply counterpressure.

Table 2. Varied factors of the DoE to determine the influence of the die movement

Factor	Unit	Range		
Punch-side sheet	mm	1.5	1.75	2.0
Die-side sheet	mm	1.5	1.75	2.0
Start time of die movement	%	35	38	41
Die velocity	mm/s	6.5	7	7.5
Die depth at start	mm	0	-0.3	-0.6

Fig. 7 shows the main-effect diagram of the investigated parameters regarding the influence of die movement on the interlock f and the minimal die-side material thickness t_r.

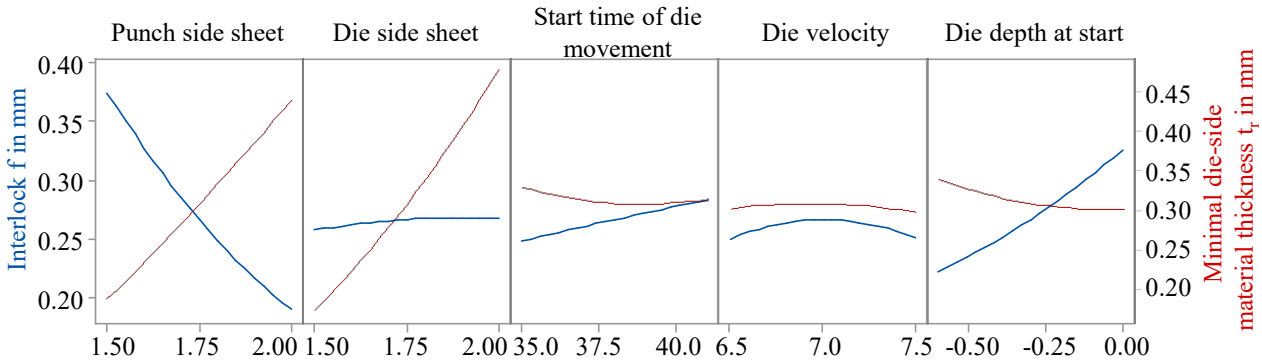

Fig. 7. Main effect diagram of the die movement parameter for the interlock f and the minimal die-side material thickness t_r related to the five parameters investigated: punch side sheet, die side sheet, start time of die movement, die velocity and die depth at start.

For the interlock, it can be seen that the sheet thickness on the punch side, the die depth at the start of the process and the timing of the die start in particular cause significant changes in the interlock. Increasing punch-side sheet thickness significantly reduces interlock (negative correlation), demonstrating that the movable die mechanism becomes critical for thick-sheet applications where conventional SPR typically fails. In contrast, the die depth at the start time has a strong positive effect on interlock formation. The lower the die depth at start time, the earlier the slug fills the rivet shank, cutting the sheet metal on the punch side earlier and increasing interlock, as shown in Fig. 8.

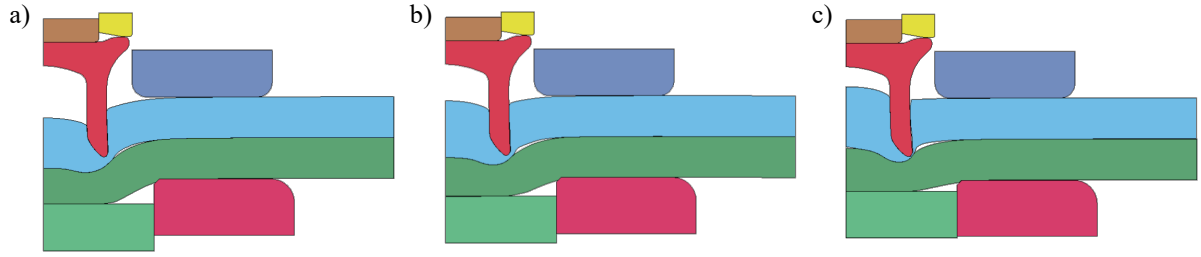

Fig. 8. Example simulations for rivet shank filling depending on the die depth at the start time, with the other factors remaining constant. a) die depth at start = -0.6 mm, b) die depth at start = -0.3 mm and c) die depth at start = 0 mm

The start time of the die movement also has a positive influence. The later the die movement begins, the greater the interlock achievable. The die-side sheet thickness and die velocity have no significant effect on interlock formation. The die-side sheet thickness has a slight positive effect. The

die velocity exhibits non-monotonic behaviour, with a medium value enabling the highest interlock, while slower and faster speeds produce lower values.

For the minimal die-side material thickness, the effect profile is partially opposite. Both sheet thicknesses, on the punch and die sides, show a significantly strong positive effect, as greater initial thicknesses favour higher minimum die-sided material thickness. In contrast to the interlock, however, a low die depth at the start of the process has a negative effect, as the rivet penetrates deeper into the material, thereby reducing the minimum die-side material thickness. The start time of the die movement shows a slight negative trend, with later movement times resulting in slightly greater thinning. The die speed has no significant effect on the residual bottom thickness. Overall, it is clear that both the die depth at the start of the process and the temporal and kinematic behaviour of the die movement are decisive for how material flow, radial expansion and thinning interact during the setting and expansion process.

For the material combination EN AW-6014 with sheet thickness a) t_1 = 1.5 mm in t_2 = 1.5 mm, b) t_1 = 1.5 mm in t_2 = 2.0 mm, and c) t_1 = 2.0 mm in t_2 = 2.0 mm, the optimisation of the die movement (red) to maximise the interlock to be achieved compared to the refence die (black), with a depth of 1.2 mm, is shown in Fig. 9.

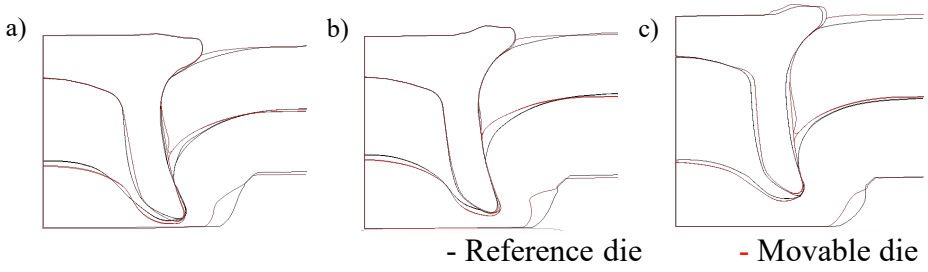

Parameter of movable die		Start time of die movement	Die velocity	Die depth at start
a	EN AW-6014, t_1 =1.5 mm, t_2 = 1.5 mm	41%	7.2071 mm/s	0.0 mm
b	EN AW-6014, t_1 =1.5 mm, t_2 = 2.0 mm	41%	6.8838 mm/s	0.0 mm
c	EN AW-6014, t_1 =2.0 mm, t_2 = 2.0 mm	41%	7.2172 mm/s	0.0 mm

Fig. 9. Joining formation of the optimisation of the movable die (red) and the reference die with a deep of 1.2 mm (black) for the material combination EN AW-6014 with sheet thickness a) t_1 =1.5 mm in t_2 = 1.5 mm, b) t_1 =1.5 mm in t_2 = 2.0 mm, and c) t_1 =2.0 mm in t_2 = 2.0 mm related to the interlock f

This shows that the die actuator enables early cutting of the punch-side sheet metal. As a result, the punch-side sheet metal is drawn in only slightly, and the die-side sheet metal forms more closely around the rivet shank, thereby increasing the interlock. However, the residual bottom thickness is minimised.

Table 3 illustrates the additional interlocking effect achievable with a movable die. For all sheet thickness combinations examined, the interlock increases significantly compared to the rigid reference die with a 1.2 mm depth. The gain is particularly pronounced at higher package thicknesses: while an increase of around 27.6 % is already achieved with the thinnest combination (1.5 / 1.5 mm), the interlock increases by more than 51.8 % with the 1.5 / 2.0 mm configuration. A similarly strong increase is observed for the thickest combination (2.0/2.0 mm), which still achieves a substantial 49.1 % enhancement. This clearly shows that the active die movement significantly improves the material flow during the setting process and unlocks considerable optimisation potential, especially with thicker sheet combinations.

Table 3. Optimisation potential of the interlock achieved by the active die actuator compared to reference joints

	Combination	Interlock f, die depth 1.2 mm	Interlock f, movable die	Procent
a	EN AW-6014, t_1 =1.5 mm, t_2 = 1.5 mm	0.2843 mm	0.3628 mm	+ 27.6 %
b	EN AW-6014, t_1 =1.5 mm, t_2 = 2.0 mm	0.2987 mm	0.4535 mm	+ 51.8 %
c	EN AW-6014, t_1 =2.0 mm, t_2 = 2.0 mm	0.1398 mm	0.2085 mm	+ 49.1 %

Table 4 shows the resulting reduction in the minimum die-side material thickness as a result of interlock optimisation through the use of an active movable die. For all sheet thickness combinations examined, a significant decrease in the minimum die-sided material thickness is observed compared to the reference with a rigid die and a depth of 1.2 mm. This effect is most pronounced in the thinnest combination (1.5/1.5 mm), where the minimum die-side material thickness is reduced by around 40.6 %. For the 1.5/2.0 mm combination, the reduction is around 18.2 %, while for the thickest combination (2.0/2.0 mm), it is comparatively moderate at around 9.8 %. This clearly shows that the increase in interlock achieved by active die movement is accompanied by greater thinning of the die-side sheet metal, with this trade-off particularly pronounced in thinner sheet material combinations. The 40.6 % reduction in minimum die-side thickness for the 1.5/1.5 mm combination approaches failure-critical levels. According to DVS 3410 guidelines, t_r should typically exceed 0.2·for reliable joint strength [5].

Table 4. Resulting reduction in minimum die-sided material thickness through optimisation of the interlock by active die actuators

	Combination	Minimum die-side material thickness t_r, die depth 1.2 mm	Minimum die-side material thickness t_r, movable die	Procent
a	EN AW-6014, t_1 =1.5 mm, t_2 = 1.5 mm	0.1449 mm	0.0861 mm	- 40,6 %
b	EN AW-6014, t_1 =1.5 mm, t_2 = 2.0 mm	0.3521 mm	0.2881 mm	- 18,2 %
c	EN AW-6014, t_1 =2.0 mm, t_2 = 2.0 mm	0.6957 mm	0.6278 mm	- 9,8 %

Fig. 10 shows the force-time diagram of the die bottom during the inner punch movement of the optimised die movements. At the beginning, the force increases at a constant die depth of zero for the three material combinations to an approximately equal level of between 18.7 kN and 19.3 kN. For the material thickness combination, a) t_1 = 1.5 mm, t_2 = 1.5 mm, the force drops to approximately 8.9 kN when the die movement starts and is kept constant until the final die depth of 1.2 mm is reached. Similar force levels result for the material thickness combination b) t_1 = 1.5 mm in t_2 = 2.0 mm. When the die movement starts, the force drops to approximately 8.3 kN, which remains constant until the end of the die movement. As with the material thickness combination c) t_1 = 2.0 mm, t_2 = 2.0 mm, the force here drops to an almost constant level of 7.6 kN. Once the maximum die depth of 1.2 mm is reached, there is a sharp increase in the force on the die bottom. The maximum force, which is between 33 and 36 kN, is reached at the maximum inner punch stroke. The evaluation of the resultant forces at the die bottom shows that the cutting process of the punch-side sheet metal has no effect on the resultant forces.

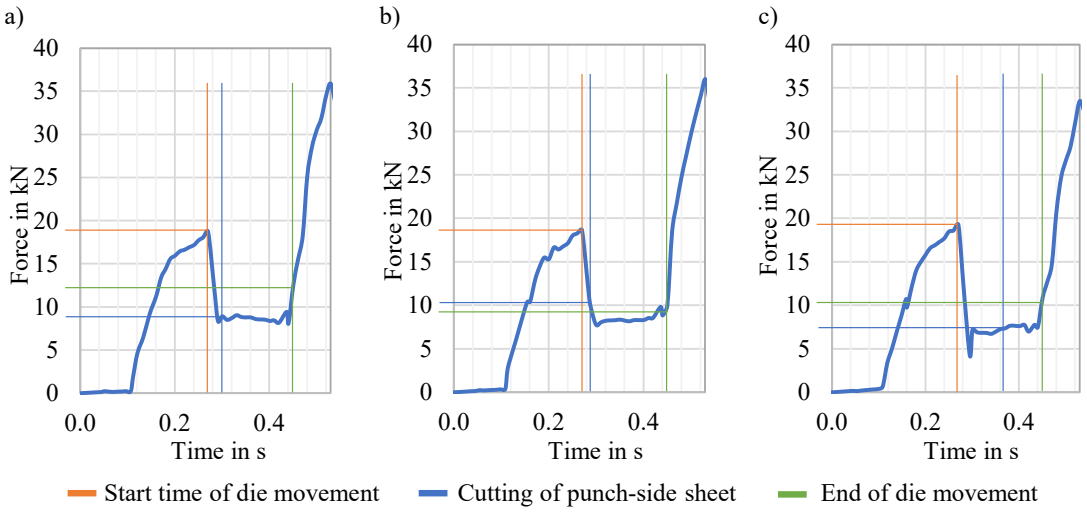

Fig. 10. Force-time diagram of the die base during movement of the inner punch for the material combination EN AW-6014 with sheet thickness a) t_1 =1.5 mm in t_2 = 1.5 mm, b) t_1 =1.5 mm in t_2 = 2.0 mm, and c) t_1 =2.0 mm in t_2 = 2.0 mm

In this strategy, the movement is initiated once the predefined force threshold is reached. The control system then maintains this force by lowering the movable die until either the maximum die depth is attained or the process kinematics prevent further die travel. For the material combination EN AW-6014 with sheet thickness a) t_1 = 1.5 mm in t_2 = 1.5 mm, forces of 18.72 kN and a force 20 % higher at 22.46 kN were selected. For the material combination EN AW-6014 with sheet thickness c) t_1 = 2.0 mm in t_2 = 2.0 mm, forces of 19.27 kN and a force 20% higher at 23.12 kN were selected. The joint formed by force-controlled die movement in green, which aims to maximise the interlock, compared with the reference die in black with a depth of 1.2 mm, is shown in Fig. 11.

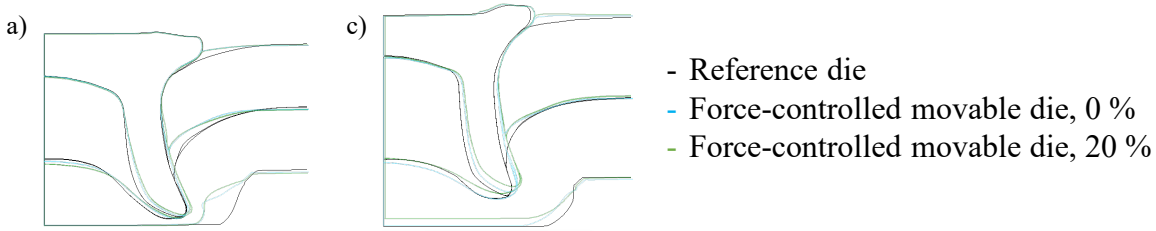

Fig. 11. Joining formation of the force-controlled movable die (blue 0 % and green 20 %) and the reference die with a deep of 1.2 mm (black) for the material combination EN AW 6014 with sheet thickness a) t_1 = 1.5 mm in t_2 = 1.5 mm and c) t_1 = 2.0 mm in t_2 = 2.0 mm related to the interlock f

Fig. 12 presents the force–time response of the force-controlled movable die during the inner punch stroke. Initially, the force increases at zero die penetration until the respective setpoint is reached. The controlled force levels correspond to 18.72 kN (a) and 22.46 kN (b) for t_1 = 1.5 mm / t_2 = 1.5 mm, and 19.27 kN (c) and 23.12 kN (d) for t_1 = 2.0 mm / t_2 = 2.0 mm. After the onset of the die motion, the force is approximately constant until the end of the die movement. The cutting operation on the punch-side sheet does not result in a noticeable change in the force response. For cases (a) and (b), the maximum die depth is reached, which results in a pronounced force increase during the subsequent inner punch stroke. In contrast, for (c) and (d), the movable die does not reach the maximum die depth due to the intensified radial material flow.

Force control positively affects the formation of the interlock. As the set force increases, the interlock form increases. As shown in Fig. 11 c), a significantly increased radial material flow results in a lower force acting on the die base, meaning that the maximum die depth is not reached, see Fig. 12 c) and d). Overall, the pronounced radial material flow has a favourable effect on the required die depth and the maximum joining force, but can potentially negatively impact adjacent joining points due to the sheet metal's radial expansion on the die side.

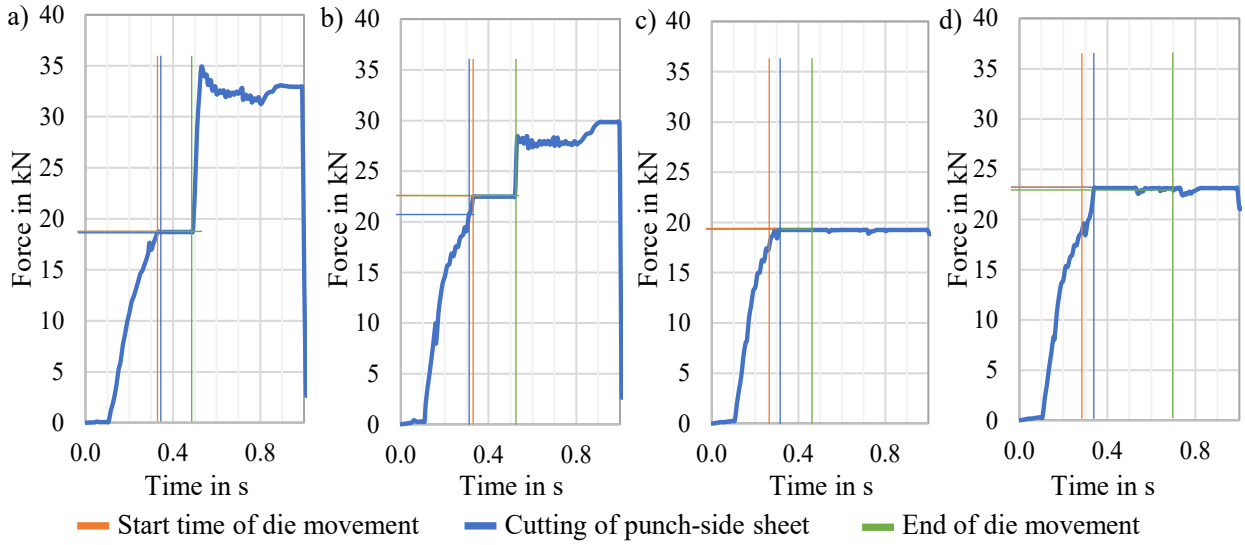

Fig. 12. Force-time diagram of the force-controlled movable die during movement of the inner punch for the material combination EN AW-6014 with sheet thickness a) t_1 =1.5 mm in t_2 = 1.5 mm with forces of 18.72 kN b) t_1 =1.5 mm in t_2 = 1.5 mm with forces of 22.46 kN, c) t_1 =2.0 mm in t_2 = 2.0 mm with forces of 19.27 kN and d) t_1 =2.0 mm in t_2 = 2.0 mm with forces of 23.12 kN

Summary

This study presents a numerical investigation of versatile self-piercing riveting (V-SPR) with a movable die, aiming to expand the process window and improve joint formation compared to conventional setups with rigid dies. A two-dimensional axisymmetric finite-element model was developed in LS-Dyna, incorporating deformable rivets and sheets as well as a kinematically controlled die base. The model was experimentally validated using EN AW-6014 sheet combinations, demonstrating high agreement in deformation behaviour and quality-relevant parameters, such as interlock and minimum die-side thickness.

A full-factorial parameter study examined the influence of punch-side and die-side sheet thickness, die depth at process start, die velocity, and the start time of die movement on joint formation. The results show that interlock formation is strongly governed by the punch-side sheet thickness, the initial die depth, and the die start time, while die velocity and die-side thickness have only minor effects. For the remaining die-side material thickness, both sheet thicknesses exert the largest influence, whereas a low die depth at the beginning of the process promotes increased thinning. Comparative simulations between a fixed die and a movable die demonstrate substantial optimisation potential. Depending on the sheet thickness combination, the interlock increases between 27.6% and nearly 52% when using an active die movement. However, this improvement is directly associated with a reduction in the minimum die-side material thickness. Compared to the rigid reference die, the minimum die-side thickness decreases significantly across all investigated combinations, with the greatest reduction observed in thin-sheet packages. While the thickest combination (2.0/2.0 mm) shows only a moderate decrease of around 9.8 %, the thinning becomes critical for thinner configurations, reaching reductions of up to 40.6 % for the 1.5/1.5 mm combination. This highlights a clear trade-off between enhanced interlock formation and increased die-side sheet thinning, which is particularly pronounced for thin sheet materials. The evaluation of the forces on the die bottom during the adjustment process also shows that the characteristic force development is largely independent of the sheet thickness combination. In all configurations, the force on the die base increases to approximately 18 to 19 kN before the die movement begins. As soon as the die begins to move, the force drops to an almost constant level, between 7.6 kN and 8.9 kN, depending on the material combination, and remains stable until the final die depth is reached. Only after the maximum tool displacement has been reached does the force increase sharply again, reaching a peak value

between 33 kN and 36 kN at full inner punch stroke. It is noteworthy that cutting the sheet metal on the punch side has no measurable influence on the resulting tool forces. Building on the force-time response shown in Fig. 10, a force-controlled die-movement strategy was investigated. Here, the motion is initiated once a defined force threshold is reached, and the controller maintains this force by lowering the die base until either the maximum die depth is achieved or the process kinematics limit further die travel. Increasing the set force increases the interlock, while the force response remains largely unaffected by cutting the punch-side sheet. For the thicker sheet package (t_1 = 2.0 mm / t_2 = 2.0 mm), intensified radial material flow reduces the force acting on the die base, preventing the maximum die depth from being reached, thereby reducing both the required die depth and the maximum joining force. At the same time, the pronounced radial expansion of the die-side sheet may influence adjacent joining points.

The results confirm that a controlled die displacement significantly enhances material flow and rivet expansion, particularly for thicker sheet packages, enabling more robust and versatile SPR joint formation. Building on these results, future work should focus on experimentally validating the identified parameter interactions across a broader range of material combinations and sheet thicknesses.

Acknowledgement

Funded by the Deutsche Forschungsgemeinschaft (DFG, German Research Foundation) – TRR 285/2 – Project-ID 418701707. The authors thank the German Research Foundation for their organisational and financial support. Data regarding the contents of the publication can be requested at www.trr285.de.

References

[1] F. Kappe, "Wandlungsfähiges Halbhohlstanznieten mit linearer Prozesskinematik," Dissertation, Shaker Verlag, 2025.

[2] F. Kappe, S. Wituschek, V. de Pascalis, M. Bobbert, M. Lechner, and G. Meschut, "Numerical Investigation of the Influence of a Movable Die Base on Joint Formation in Semi-tubular Self-piercing Riveting," in Materials Design and Applications IV (Advanced Structured Materials), L. F. M. Da Silva, Ed., Cham: Springer International Publishing, 2023, pp. 137–149.

[3] European Commission. "Delivering the European Green Deal." [Online]. Available: https://commission.europa.eu/topics/climate-action/delivering-european-green-deal_en

[4] K. Martinsen, S. J. Hu, and B. E. Carlson, "Joining of dissimilar materials," CIRP Annals, vol. 64, no. 2, pp. 679–699, 2015, doi: 10.1016/j.cirp.2015.05.006.

[5] Technical Bulletin DVS 3410: Self-pierce Riveting - Overview., European Research Association for Sheet Metal Working, Düsseldorf, 2019.

[6] Donhauser G, Mauermann R, Quaißer G et al, “Stamping rivet upsetting tool comprises die endface which is radially divided into sectors outside raised area,” DE19847980 A1.

[7] W. G. Drossel and M. Jäckel, "New Die Concept for Self-Pierce Riveting Materials with Limited Ductility," KEM, vol. 611-612, pp. 1452–1459, 2014, doi: 10.4028/www.scientific.net/KEM.611-612.1452.

[8] Saarstahl. "Werkstoff-Datenblatt Saarstahl C35R." Accessed: Feb. 12, 2024. [Online]. Available: https://www.saarstahl.com/sag/downloads/download/9082

[9] Novelis Global Automotive, Datasheet: Novelis AdvanzTM 6F - e170.

[10] F. Kappe, S. Wituschek, M. Bobbert, and G. Meschut, "Determining the properties of multi-range semi-tubular self-piercing riveted joints," Prod. Eng. Res. Devel., vol. 16, 2-3, pp. 363–378, 2022, doi: 10.1007/s11740-022-01105-2.

[11] F. Kappe, C. Zirngibl, B. Schleich, M. Bobbert, S. Wartzack, and G. Meschut, "Determining the influence of different process parameters on the versatile self-piercing riveting process using numerical methods," Journal of Manufacturing Processes, vol. 84, pp. 1438–1448, 2022, doi: 10.1016/j.jmapro.2022.11.019.

[12] Self-piercing riveting: Properties, processing and applications (Woodhead publishing series in welding and other joining technologies 82). Oxford: WP Woodhead Publ, 2014